SUPPLEMENTAL METHODS

Loss-of-function studies. The 4 shRNA pLKO.1 set were purchased from Open Biosystem (Thermo Scientific, Inc.). Of the 4 shRNA set, shRNAs number 3 (shRNA A) and 1 (shRNA B) resulted the most efficient in silencing JARID1C expression. They have the following hairpin sequences and both recognize the coding sequence of human JARID1C:

shRNA A:

*CCGG***GTGACAGTAAACGGCACCT***TTCTCGAGAA***AGGTGCCGTTTACTGT CA***CTTTT***

shRNA B:

*CCGG***GCAGTGTAACACACGTCCA***TTCTCGAGAA***TGGACGTGTGTTACAC TG***CTTTT***

Common structures of shRNA backbones are higlighted in italics. Of note, shRNAs A and B targeted and silenced also the murine homologue of human JARID1C, despite one nucleotide mismatch (shRNA A) inside the sequence or some mismatches (shRNA B) at the 3' of the murine target sequence. Non-targeting, scrambled shRNA (CTR shRNA) negative control was purchased from Sigma.

Studies in NIH-3T3 cells were performed by transfection with jetPRIME™ (Polyplus Transfection) according to the manufacturer instructions. 72 hours p. t. total cell lysates and cells for immunofluorescence were obtained. Loss-of-function studies in Caki-1, A498 and MEFs were performed by transduction of cells with pLK0.1 lentiviral vectors containing shRNAs targeting KDM5C/JARID1C. Puromycin selection (Sigma) was performed at 2.5 μg/ml, starting 18-24 hours after the transduction and lasting 72 hours. For lentivirus production, HEK293T (clone #17,

ATCC) were transfected with the $CaCl_2$ method. To this end, a mix containing: 10 μg of transfer vector, 6.5 μg of packaging vector Δr 8.74, 3.5 μg of Env VSV-G, 2.5 μg of REV, 300 μl of 0.1X TE, 150 μl of dH2O, 50 μl of 2.5M $CaCl_2$ and 500 μl of 2X HBS was added drop by drop on a $10cm^2$ dish. After 18 hours the medium was changed and after other 36 hours the medium was collected and ultracentrifuged. The pellet of viral particles was resuspended in PBS and stored at –80°C in small aliquotes to avoid freeze-thaw cycles.

Plasmids. JARID1C cDNA (pCMV-SPORT6 expression vector, Open Biosystems) was cloned in a MSCV vector backbone (Addgene) and used for mammalian expression experiments. FLAG-$SMCX_{long}$ was kindly provided by Professor Ralf Janknecht (University of Oklahoma Health Sciences Center, Oklahoma City, OK, USA); myc-SUV39H1 was a generous gift from Professor Thomas Jenuwein (Max Planck Institute of Immunobiology and Epigenetics, Freiburg, Germany) while HA-DDB1 was a generous gift from Dr Michel Strubin (Centre Médical Universitaire, Geneve, Switzerland).

Immunofluorescence. For BrdU analysis of S phase cells, 48 hours after transfection with shRNA-coding plasmids, 20^4 NIH3T3 or HeLa cells were transferred in 24 multiwell plates with 13 mm glass coverslips (Ettore Pasquali). 24 hours after, cells were 30 minutes pulsed with BrdU, twice washed in PBS and fixed in 4% Paraformaldeyde (PFA, Sigma) for 10 minutes at RT. Then, cells were permeabilized with 0.3% Triton X-100 (Sigma) in PBS for 10 minutes at RT. After three PBS washes, aspecific sites were blocked by treatment with PBS/3% BSA (blocking solution) for 30 minutes at RT. Staining with anti-BrdU primary antibody was performed for 1 hour at RT and was prepared in blocking solution by adding DNase (Qiagen) at 37 μL/mL and 3 mM $MgCl_2$. Anti-FLAG antibody was used to detect FLAG-$SMCX_{long}$. Anti-mouse secondary antibody was prepared in PBS/3% BSA that was left 45 minutes at RT. Coverslips were mounted on glass slides with ProLong® Gold Antifade Reagent with DAPI (Invitrogen) and analyzed with AxioImager A2

fluorescent microscope (Zeiss). For BrdU analysis of S phase cells, 150 cells per condition (CTRsh e J1Csh) were examined and the BrdU pattern classified as early, medium or late based on (1). For MEFs, $15*10^3$ early passage (P4-P5) cells were plated on 13 mm glass coverslips (Ettore Pasquali) and left to attach overnight. The day after, cells were fixed. Staining was performed as for BrdU except that primary antibody was anti- α -tubulin (Sigma) and no DNase/$MgCl_2$ was included. For quantification of instability events, about 200 cells per condition per experiment (CTRsh and J1CshA) were counted. To analyse DAPI intense foci, NIH3T3 cells transduced with CTRsh or J1C shA were plated soon after puromycin selection at 15^4 /each of 24 multiwells. The day after, fixing with PFA was followed by permeabilization with Triton X-100 and mounting/staining with ProLong® Gold Antifade Reagent with DAPI (Invitrogen). About 100 cells per condition and for each experiment were analysed. For FLAG-JARID1C immunofluorescence on NIH3T3 cells, colocalization with DAPI intense foci was analized at the Leica Confocal – TCS SP2 Laser Scanning Confocal at the Alembic (Advanced Light and Electron Microscopy Bio-Imaging Centre) San Raffaele Institute. Representative images depicted in Fig. 1-4 were obtained at the Leica Confocal – TCS SP2 Laser Scanning Confocal as well.

CSK fractionation. Triton X-100 extraction on NIH3T3 was performed as in (2). Briefly, release of chromatin-bound material was performed in multiwell plates by extraction with 0.5%T CSK (10 mM PIPES pH 7, 100 mM NaCl, 300 mM sucrose, 3 mM MgCl2) for 5 minutes. Cells were then rinsed with CSK and PBS before fixation in 4% PAF. Protease and phosphatase inhibitors were included during extraction and following rinses.

SDS-PAGE and immunoblotting. Cells pellets were washed twice with ice-cold PBS, resuspended in Laemmli Sample Buffer 1X + 100mM DTT and sonicated with

five x 1 minute 30'' ON/30'' OFF cycles with Bioruptor (Diagenode). Proteins were electrophoretically separated with polyacrylamide gels (BioRad) and transferred to nitrocellulose membrane (GE Healthcare, Amersham Hybond ECL) with a Mini Trans–Blot Electrophoretic Transfer System (Biorad).

RNA extraction and Real Time (RT)-PCR. Total RNA was isolated using Trizol (Invitrogen, Carlsbad, CA, USA) according to the manufacturer's instruction. Briefly, cells were resuspended in Trizol and phases separated using 1-Bromo-3-chloropropane. Total RNA from the aqueous phase was precipitated with isopropanol overnight. The day after, pellet was washed with 75% ethanol and resuspended in RNAse-free water. DNase (Qiagen) treatment was performed at 37°C for 45 minutes and DNA-free RNA was purified with RNeasy Micro/ Mini Kit (Qiagen). Elution from columns was performed in 20-30 µl of RNAse-free water. RNA concentration and purity was evaluated with a spectrophotometer (Nanodrop, Thermo Scientific). cDNA was generated according to First-Strand cDNA Synthesis by using SuperScript™ III RT Protocol (Invitrogen), with random primers. Real-time PCR was performed using Sybr Green Master Mix (Applied Biosystems) on the Viia 7 Real Time PCR System (Applied Biosystems). The output was analysed with ΔΔCt method and normalised on the expression of GAPDH. Primers are listed below.

	Forward	**Reverse**
murine JARID1C	CACTGTGGTAAGCACGAGGA	CTCGTCACCCTCATGAATCC
GAPDH	AGCCACATCGCTCAGACAC	GCCCAATACGACCAAATCC
murine GAPDH	AATGTCAGCAATGCATCCTG	ATGGACTGTGGTCATGAGCC
minor (5)	CATGGAAAATGATAAAAACC	CATCTAATATGTTCTACAGTGTGG
major (5)	GACGACTTGAAAAATGACGAA	CATATTCCAGGTCCTTCAGTGTGC

	ATC	
LINEL1 (5)	TTTGGGACACAATGAAAGCA	CTGCCGTCTACTCCTCTTGG
SINEB1 (5)	GTGGCGCACGCCTTTAATC	GACAGGGTTTCTCTGTGTAG
SINEB2 (5)	GAGATGGCTCAGTGGTTAAG	CTGTCTTCAGACACTCCAG
Chrom 1 α SAT (4)	TCATTCCCACAAACTGCGTTG	TCCAACGAAGGCCACAAGA
pericentric SATα (4)	AAGGTCAATGGCAGAAAAGAA	CAACGAAGGCCACAAGATGTC

All primers were used at a final concentration of 400 nM excepts major that were used 200 nM.

Immunoprecipitation. Every experiment was performed with at least $15x10^6$ cells. All protein purifications were carried out on cell nuclei prepared by 20 min swelling in nuclear prep buffer (10mM Tris-HCl pH 7.6, 100mM NaCl, 2mM MgCl2, 0.3 M Sucrose, 0.25 % v/v Igepal) at 4°C. After 8' of incubation on ice and a 10', 6100rpm, 4°C centrifugation, nuclei were lysed in high salt buffer (20mM Tris–HCl pH 7.5, 300mM NaCl, 10% glycerol, 0.25% Igepal) (3) with fresh addition of a protease inhibitor cocktail (Roche). The lysate was incubated 45' on ice, then ultracentrifuged 1 hour, 15000 rpm, 4°C. The supernatant was split in two, half of which added with specific antibody while the other half with control isotipic IgG and put on the wheel overnight, 4°C, after addition of 50 µl of PBS-washed protein A/G agarose slurry beads (Calbiochem). The 3% of the supernatant used for in the reactions was resuspended in Laemmli 1X (Total Input). The morning after, the mixture was washed 4/5 times with Lysis Buffer + 0,1% Tween (500-700 µl / each). Then, final elution step with Laemmli 1X, 25-30 µl/IP, 15'at RT. The eluted supernatant represents the immunoprecipitate (IP).

Chromatin ImmunoPrecipitation (ChIP). Chromatin was collected and purified as in (4). LB1, LB2 and LB3 were supplemented with Complete, EDTA-free Protease Inhibitor Cocktail Tablets (Roche) and the phosphatase inhibitors sodium orthovanadate and NaF. Lysates were sonicated with Bioruptor (Diagenode). Briefly, 300 µL aliquots of LB3 lysates were put in Eppendorf 1,5 mL tubes and sonicated for 10' (medium intensity 30'' on 30'' off). Fragment length was considered of good quality when enriched in fragments of 300-500 bp. Upon spectrophotometric quantification of chromatin (Nanodrop), 50-100 μg of ready-to-use chromatin were used for each anti-humanJARID1C ChIP, while 10-20 μg were used for each ChIP to histones. For each ChIP, 70 μl of Dynabeads protein G slurry (Invitrogen) were washed and incubated with 10 μg of antibody (5 μg in ChIPs to histones). Samples were purified with QIAquick PCR purification kit (Qiagen), following manufacturer's recommendations. DNA was eluted in 50 μl of TE buffer and 1-2 μl were used in qPCR Sybr® Green qPCR kit (Invitrogen).

ChIP q-PCR analysis. To determine the enrichment obtained, we normalized ChIP-qPCR data for input chromatin (reported as % input in the Figures).

	Forward	**Reverse**
BDNF (8)	AGAGCCAACGGATTTGTC	CTTGCCAAGAGTCTATTCC
SYN1 (8)	TGGGTTTTAGGACCAGGATG	GGTGCTGAAGCTGGCAGT
major (9)	AAATACACACTTTAGGACG	TCAAGTGGATGTTTCTCATT
minor (9)	GAAAATGATAAAAACCACAC	ACTCATTGATATACACTGTT
Chrom 1 α SAT (3)	TCATTCCCACAAACTGCGTTG	TCCAACGAAGGCCACAAGA
Chrom 4 α SAT (3)	CTGCACTACCTGAAGAGGAC	GATGGTTCAACACTCTTACA
SATI pericentric (3)	TCATTCCCACAAACTGCGTTG	TCCAACGAAGGCCACAAGA

SATII pericentric (3) TGAATGGAATCGTCATCGAA CCATTCGATAATTCCGCTTG

All primers were used at a final concentration of 400 nM.

Correlation of chromatin modifications and JARID1C. We downloaded raw sequences belonging to SRA study SRP010385 (GSE32509), aligned to reference genome hg19 with bwa aligner (5). We built IP profiles from alignments and calculated pair-wise correlations using wigCorrelate tool (6).

Differential analysis of H3K4me3 signal in JARID1C silenced mice. We defined heterochromatic regions in ES-E14 cell lines using available ENCODE data on DNAseI hypersensitivity sites and H3K9me3 ChIP. DNAseI peaks were sloped up to 5 kb upstream and downstream; overlapping intervals were then merged. The complement of such domains over the genome was considered DNAseI free sites. H3K9me3 signal was smoothed with a running Hanning filter implemented in dspchip (https://code.google.com/p/dspchip/). H3K9me3 domains were then identified from smoothed signal. Intersection between H3K9me3 domains and DNAseI free sites were considered *bona fide* heterochromatic regions. We downloaded raw sequences for H3K4me3 from SRA study SRP010203 (GSE34975) and aligned to reference genome mm9 using bwa aligner. We then counted H3K4me3 reads over heterochromatic domains previously defined. We used TMM normalization implemented in edgeR with a Acutoff=-12. Normalized counts were then used to extract FPKM values for all domains. Statistical significance of the difference was assessed with Kolmogorov-Smirnoff test.

Analysis of ChIP-seq. Read tags were aligned to hg19 reference genome using bwa aligner (v 0.7.5, [1]). Each aligner was processed with MACS (v 2.10.0, [2]) with two sets of parameters in order to identify narrow peaks and broad domains. In particular, narrow peaks were identified for H3K4me1, H3K4me3, H3K9me3 and KDM5C

markers using Input DNA as control and default parameters. Broad domains were identified for H3K4me1, H3K9me3 and KDM5C markers enabling the 'broad' option and setting a broad-cutoff to 0.2. Narrow peaks were analyzed with IDR (v 2.0.1, [3]) setting a IDR threshold of 540 as cutoff to define consistent peaks between replicates.

In order to identify trustable broad domains, we performed cutoff analysis (implemented in MACS) to determine an optimal p-value cutoff for such regions. In order to to this we looked at the first inflection point in the curve pscore/npeaks in MACS output. Once such score was automatically chosen, we filtered broad domains for a pvalue higher than the threshold (table?). Filtered domains from each couple of replicates were then clustered using clustering functions implemented in bx-python suite (https://bitbucket.org/james_taylor/bx-python/wiki/Home), allowing for a maximal distance between regions of 10 kbp. Since we could identify a high number of summits in H3K4me1 and H3K9me3 signals, we clustered those narrow peaks allowing for a maximal distance of 50 kbp. We then used these latter to refine broad clusters formely identified. Correlation between ChIP-seq signal was assessed with wigCorrelate tool (part of the UCSC utilities, [4]), clipping values to 200 in order to avoid spurious correlations. Heatmap was generated using R package pheatmap.

Assessment of significative associations betweek KDM5C domains and other markers was performed with GenometriCorr R/Bioconductor package ([5])

Figure 1A was generated using denoised ChIP-seq signals, processed with dspchip tool (https://code.google.com/p/dspchip/). Briefly, each signal was smoothed using Hanning filter (expected signal size 65kbp) after signal normalization, Input track was subtracted by each IP track and negative values were removed.

Hilbert Curve Visualization. Hilbert Curve Visualization (HCV) of ChIP-Seq data was generated using in house scripts (gilbert, available at https://bitbucket.org/dawe/gilbert), according previous reports (7). The Hilbert plots represent linear sequence data visualized in two-dimensional space, where each

colored spot is proportional to the signal intensity in the corresponding genomic region. Images for single chromosomes were imported in ImageJ and processed by equalization and subtraction of input signals. Single channels (Yellow= Jarid1C, Magenta=H3K9me3, Cyan=H3K4me1 Gray= H3K4me3) were then merged to generate the overlay plots.

Generation of JARID1C mutant and rescue experiments. MSCV-wtJARID1C vector was used as template plasmid to build up double H514A/A388P mutant by two different rounds of site-directed mutagenesis, as based on the kit protocol from Stratagene. Briefly, for each round, 5, 10, 20 and 50 ng of template plasmid were used for PCR with mutated primers (sequences are listed below). After the site-directed mutagenesis reaction, parental, methylated plasmid was destroyed by DpnI digestion. 5 to 10 μL of PCR-mutated plasmids were used to transform 100 μL of Mach1® competent cells (Invitrogen). Plasmid DNA of grown colonies was extracted and verified through sequencing at Primm Srl, Milan. Colonies containing mutated plasmid were then glycerol-stocked and a Maxi-Prep was prepared for transfection experiments. For the second round of site-directed mutagenesis, A388P mutated primers (listed below) were used with the MSCV-H514A single mutant backbone as a template. Rescue experiments were performed by transient transfection with shRNA plasmids. Briefly, pLKO.1 containing scrambled and JARID1C specific (shRNA A) shRNA hairpins were transfected with *jetPRIME™* . 24 hours after, 250 ng of MSCV-LacZ, MSCV-wtJARID1C or MSCV-mutant (H514A/A388P) were transfected for each 6 well plate. Together with rescue plasmids, an unmatched GFP-encoding plasmid was transfected to reach the right 1:3 *jetPRIME™* DNA ratio. After 48 hours from rescue

Forward

GGTCTTCTCAGCCTTTTGCTGGGCTATTGAGGATCACTGGAG

H514A

Reverse

CTCCAGTGATCCTCAATAGCCCAGCAAAAGGCTGAGAAGACC

Forward

A388P

GCCTTTGGCTTTGAGCAGCCTACCCGGGAATACACTCTG

Reverse

CAGAGTGTATTCCCGGGTAGGCTGCTCAAAGCCAAAGGC

and 72 hours from pLKO.1 transfection, cells were detached, pelleted for lysates and RNA extraction.

LNA-DNA gapmers. LNA^{TM} GapmeRs against minor and major satellite repeats were designed by Exiqon's proprietary software and generated in order to achieve optimal performance. Mock LNA sequence is AACACGTCTATACGC. To target satellite repeats, we used a mix of four LNAs, two targeting minor repeats and two major. Sequences of LNAs against minor were ACTCACTCATCTAAT and TTCAGTGTAACTCAC while sequences of oligos designed against major were ACGTCCTAAAGTGTG and TTCAAGGTCGTCAAGT.

MEFs were initially transduced with lentiviral vectors encoding a control shRNA or a J1C-specific shRNA. LNA gapmers were transfected into CTRsh e J1Csh cells with jetPRIME™ (Polyplus Transfection) according to the manufacturer instructions. 72 hours post tranfection, lysates for RNA were taken and cells were PFA-fixed on glass

slides for subsequent immunofluorescence analysis (see Immunofluorescence section for instability analysis). About 120 stained cells per condition were analyzed.

DNA methylation studies on primary ccRCCs. Analysis of methylation patterns for ccRCC samples carrying JARID1C mutations was performed as in (8). Briefly, analysis was performed on Level 3 of the following datasets available at TGCA portal (http://tcga-data.nci.nih.gov/tcga/), limited to the HumanMethylation450 platform:

jhu-usc.edu_KIRC.HumanMethylation450.Level_1.1.9.0

jhu-usc.edu_KIRC.HumanMethylation450.Level_1.2.9.0

jhu-usc.edu_KIRC.HumanMethylation450.Level_1.3.9.0

jhu-usc.edu_KIRC.HumanMethylation450.Level_1.4.9.0

jhu-usc.edu_KIRC.HumanMethylation450.Level_1.5.9.0

jhu-usc.edu_KIRC.HumanMethylation450.Level_1.6.9.0

jhu-usc.edu_KIRC.HumanMethylation450.Level_1.7.9.0

jhu-usc.edu_KIRC.HumanMethylation450.Level_1.8.9.0

Level 3 data contain β-values for 482,421 CpG sites, these were filtered for those where β is not available ('NA'), resulting in 386,762 sites. A total of 292 arrays for tumor samples was included in this study. In order to address methylation changes, we performed two-sample t-test on β-values comparing JARID1C-mutant samples (n=18) versus JARID1C-wildtype samples (n=274); we applied Benjamini-Hochberg correction for multiple tests on *p-values* resulting from t-test. Finally, we called 374 significant methylation changes by applying a filter on corrected *p-values* (FDR <= 0.05). We plotted difference between the means of β-values against the nominal *p-values*, coloring dots by the corrected *p-value*. CpG sites called significant were depicted in a heatmap together with β-values from 16 arrays belonging to normal tissues for JARID1C-mutant samples.

Analysis of H3K4 methylation in adult kidney. We downloaded wiggle profiles of human adult kidney H3K4me1 ChIP-seq data from GEO (GSM773001). We extracted the maximum value in an interval of ±2500 bp around significant CpG sites. We tested the difference of data distribution between CpG sites that are hypo- or hypermethylated with Kolmogorov-Smirnoff test (D=2.71e-01, p=2.21e-05).

All statistical analyses of both DNA methylation and ChIP-seq studies were conducted with python 2.7.5, using scipy library 0.12.0 and matplotlib graphic library 1.3.0.

Patient copy number aberration and survival analysis. TCGA ccRCC patients data were downloaded from cBioPortal (9). For copy number aberration (CNA) analysis, data from 436 samples were used. The fraction of copy number altered genome represents the length of segments with log2 CNA (Copy Number Aberration) value larger than 0.2 divided by the length of all segments measured. Survival was evaluated for 411 ccRCC patients from TCGA for which survival information was available.

lncRNA differential expression analysis. lncRNA expression estimation was calculated from RNA-seq data generated by The Cancer Genome Atlas Clear Cell Renal Cell Carcinoma (TCGA KIRC) network(8). In brief, *PRADA(10)* aligned bam files were used as input files to quantify RNA expression based on gene annotation file from GENCODE v17(11). We filtered out ambiguous transcript annotations as previously described(12). We quantified combined mRNA and filtered ncRNA expression in RPKM units using *gfold count* method(13). For lncRNA differential expression analysis between JARID1C mutant (n=27) and WT (n=461) samples, we focused on 6,614 GENCODE defined long, intergenic ncRNA (lincRNA) in evolutionary conserved regions. We identified differentially expressed lincRNAs using *SAM* approach(14) at q-value of < 0.25.

Correlation between H3K9me3/H3K4me1 and lincRNAs expression. Human

adult normal kidney ChIP-seq peaks for H3K9me3 (GEO ID *GSM773026*) and H3K4me1 (GEO ID *GSM773001*) were called with MACS (v2.0.10 from (15)) using DNA input control (GEO ID *GSM773025*) using default parameters. Overlap between lincRNAs dysregulated in JARID1C-mutated samples and ChIP-seq peaks was computed using bedtools (http://www.ncbi.nlm.nih.gov/pubmed/20110278).

Antibodies. For cytofluorimetric analysis of BrdU incorporation, directly conjugated Alexa Fluor-647 antibody from BD Pharmingen was used (Cat. # 560209). Immunofluorescent analysis of S phase stages was performed with mouse anti-BrdU antibody from Becton Dickinson (Cat. # 347583). Anti-FLAG antibody was obtained from Sigma (M2 clone, Cat. # F3165). As secondary antibody, anti-mouse FITC from Molecular probes was used (Alexa Fluor-488, Cat. # A21202). For immunoblotting of nitrocellulose membrane, primary antibodies used were: α-huJARID1C (Abcam, Cat. # 72152); α-mJARID1C (Cell Signalling, Cat. # D29B9); α-HP1α (Millipore, Cat. # MAB3446); α-myc (Covance, Cat. # 616801); α-HA (Roche, clone 12CA5); α-DDB1 (Abcam, Cat. # 97522); α-H3K4me3 (Millipore, Cat. # 07-473); anti-H3K9me3 (Millipore, Cat. # 07-442). Loading control: horseradish peroxidase (HRP)- conjugated α-actin (BD Biosciences, Cat. # 612656). Secondary antibodies used were HRP- conjugated α-mouse, α-rabbit (both from GE Healthcare, Cat. # NA931 and NA934) and α-goat (Santa Cruz Biotechnology, Cat. # 2020). After immunoblotting, signals were detected using ECL Detection System (Amersham). **Co-IPs.** Antibodies used were as follows: anti-huJARID1C (Abcam Cat. # 72152, 5 µg/IP); α-HA (12CA5 Roche, 2 µg/mL of lysate); anti-HP1α (Millipore MAB3446, 1 µg/mL of lysate), anti-FLAG (Sigma M2 clone, 2 µg/mL of lysate); anti-myc (Covance, 1 µg/mL of lysate). Control isotypic IgGs were from Santa Cruz Biotechnology. **ChIPs.** Antibodies used were as follows: anti-huJARID1C (Abcam, Cat. # 72152, 10 µg/ChIP), anti-H3K4me3 (Millipore, 5 µg/IP), anti-H3K9me3

(Millipore, 5 μg/IP), anti-H3K4me1 (Abcam, 5 μg/IP). Control isotypic IgGs were from Santa Cruz Biotechnology.

SUPPLEMENTAL REFERENCES

1. Dimitrova, D.S., and Berezney, R. 2002. The spatio-temporal organization of DNA replication sites is identical in primary, immortalized and transformed mammalian cells. *Journal of cell science* 115:4037-4051.
2. Groth, A., Corpet, A., Cook, A.J., Roche, D., Bartek, J., Lukas, J., and Almouzni, G. 2007. Regulation of replication fork progression through histone supply and demand. *Science* 318:1928-1931.
3. Vella, P., Scelfo, A., Jammula, S., Chiacchiera, F., Williams, K., Cuomo, A., Roberto, A., Christensen, J., Bonaldi, T., Helin, K., et al. 2013. Tet proteins connect the O-linked N-acetylglucosamine transferase Ogt to chromatin in embryonic stem cells. *Molecular cell* 49:645-656.
4. Cabianca, D.S., Casa, V., Bodega, B., Xynos, A., Ginelli, E., Tanaka, Y., and Gabellini, D. 2012. A long ncRNA links copy number variation to a polycomb/trithorax epigenetic switch in FSHD muscular dystrophy. *Cell* 149:819-831.
5. Li, H., and Durbin, R. 2010. Fast and accurate long-read alignment with Burrows-Wheeler transform. *Bioinformatics* 26:589-595.
6. Kent, W.J., Zweig, A.S., Barber, G., Hinrichs, A.S., and Karolchik, D. 2010. BigWig and BigBed: enabling browsing of large distributed datasets. *Bioinformatics* 26:2204-2207.
7. Chandra, T., Kirschner, K., Thuret, J.Y., Pope, B.D., Ryba, T., Newman, S., Ahmed, K., Samarajiwa, S.A., Salama, R., Carroll, T., et al. 2012. Independence of repressive histone marks and chromatin compaction during senescent heterochromatic layer formation. *Mol Cell* 47:203-214.
8. 2013. Comprehensive molecular characterization of clear cell renal cell carcinoma. *Nature* 499:43-49.
9. Cerami, E., Gao, J., Dogrusoz, U., Gross, B.E., Sumer, S.O., Aksoy, B.A., Jacobsen, A., Byrne, C.J., Heuer, M.L., Larsson, E., et al. 2012. The cBio cancer genomics portal: an open platform for exploring multidimensional cancer genomics data. *Cancer discovery* 2:401-404.
10. Torres-Garcia, W., Zheng, S., Sivachenko, A., Vegesna, R., Wang, Q., Yao, R., Berger, M.F., Weinstein, J.N., Getz, G., and Verhaak, R.G. 2014. PRADA: pipeline for RNA sequencing data analysis. *Bioinformatics*.
11. Harrow, J., Frankish, A., Gonzalez, J.M., Tapanari, E., Diekhans, M., Kokocinski, F., Aken, B.L., Barrell, D., Zadissa, A., Searle, S., et al. 2012. GENCODE: the reference human genome annotation for The ENCODE Project. *Genome research* 22:1760-1774.
12. Akrami, R., Jacobsen, A., Hoell, J., Schultz, N., Sander, C., and Larsson, E. 2013. Comprehensive analysis of long non-coding RNAs in ovarian cancer reveals global patterns and targeted DNA amplification. *PloS one* 8:e80306.
13. Feng, J., Meyer, C.A., Wang, Q., Liu, J.S., Shirley Liu, X., and Zhang, Y. 2012. GFOLD: a generalized fold change for ranking differentially expressed genes from RNA-seq data. *Bioinformatics* 28:2782-2788.
14. Tusher, V.G., Tibshirani, R., and Chu, G. 2001. Significance analysis of microarrays applied to the ionizing radiation response. *Proceedings of the National Academy of Sciences of the United States of America* 98:5116-5121.
15. Zhang, Y., Liu, T., Meyer, C.A., Eeckhoute, J., Johnson, D.S., Bernstein, B.E., Nusbaum, C., Myers, R.M., Brown, M., Li, W., et al. 2008. Model-based analysis of ChIP-Seq (MACS). *Genome biology* 9:R137.

16. Ram, O., Goren, A., Amit, I., Shoresh, N., Yosef, N., Ernst, J., Kellis, M., Gymrek, M., Issner, R., Coyne, M., et al. 2011. Combinatorial patterning of chromatin regulators uncovered by genome-wide location analysis in human cells. *Cell* 147:1628-1639.
17. Outchkourov, N.S., Muino, J.M., Kaufmann, K., van Ijcken, W.F., Groot Koerkamp, M.J., van Leenen, D., de Graaf, P., Holstege, F.C., Grosveld, F.G., and Timmers, H.T. 2013. Balancing of histone H3K4 methylation states by the Kdm5c/SMCX histone demethylase modulates promoter and enhancer function. *Cell reports* 3:1071-1079.
18. Dalgliesh, G.L., Furge, K., Greenman, C., Chen, L., Bignell, G., Butler, A., Davies, H., Edkins, S., Hardy, C., Latimer, C., et al. 2010. Systematic sequencing of renal carcinoma reveals inactivation of histone modifying genes. *Nature* 463:360-363.

SUPPLEMENTAL FIGURES AND FIGURE LEGENDS

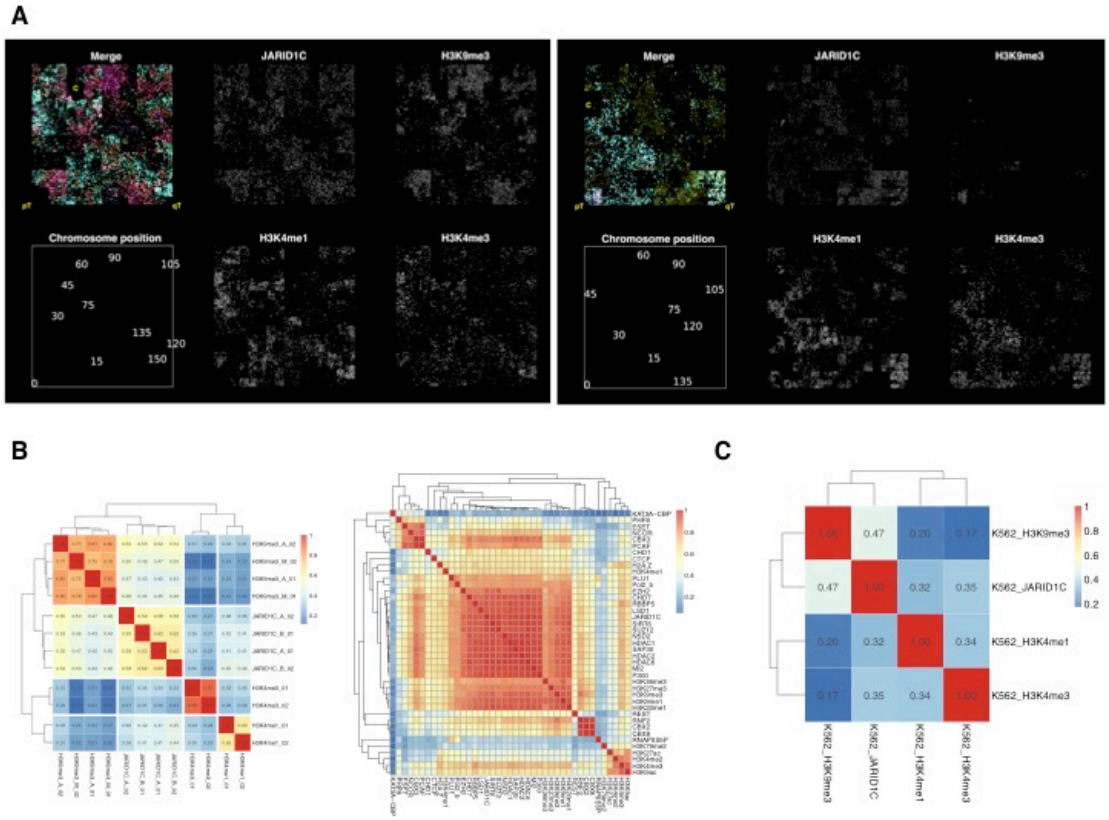

Figure S1. **A**, Hilbert Curve representation of multiple ChIP-seq profiles on chromosome 8 (top) and chromosome X (bottom). Multiple markers were assigned to color channel before merge (JARID1C Yellow; H3K9me3 Magenta; H3K4me1 Cyan; H3K4me3 Gray). Merged image is annotated with both telomere positions (pT and qT) and centromere (c); H3K9me3 signal are scarcely enriched on chromosome 8, revealing the absence of aspecific JARID1C signal that would appear as bright yellow spots. **B**, Heatmap showing correlation between multiple ChIP-seq signals discussed in the main text. Here biological duplicates are presented separately. A good correlation is found among different runs of the same antibody; high correlation between JARID1C and H3K9me3 can be observed. **C**, Heatmap showing correlation between multiple ChIP-seq signals as from K562 cell line (16). Heatmap on the left shows the correlation among a wide variety of chromatin associated proteins and histone modification. A central cluster, including JARID1C, can be associated to chromatin silencing. Heatmap on the right, a subset of K562 data, shows the correlation of JARID1C with histone modifications also discussed in the main text.

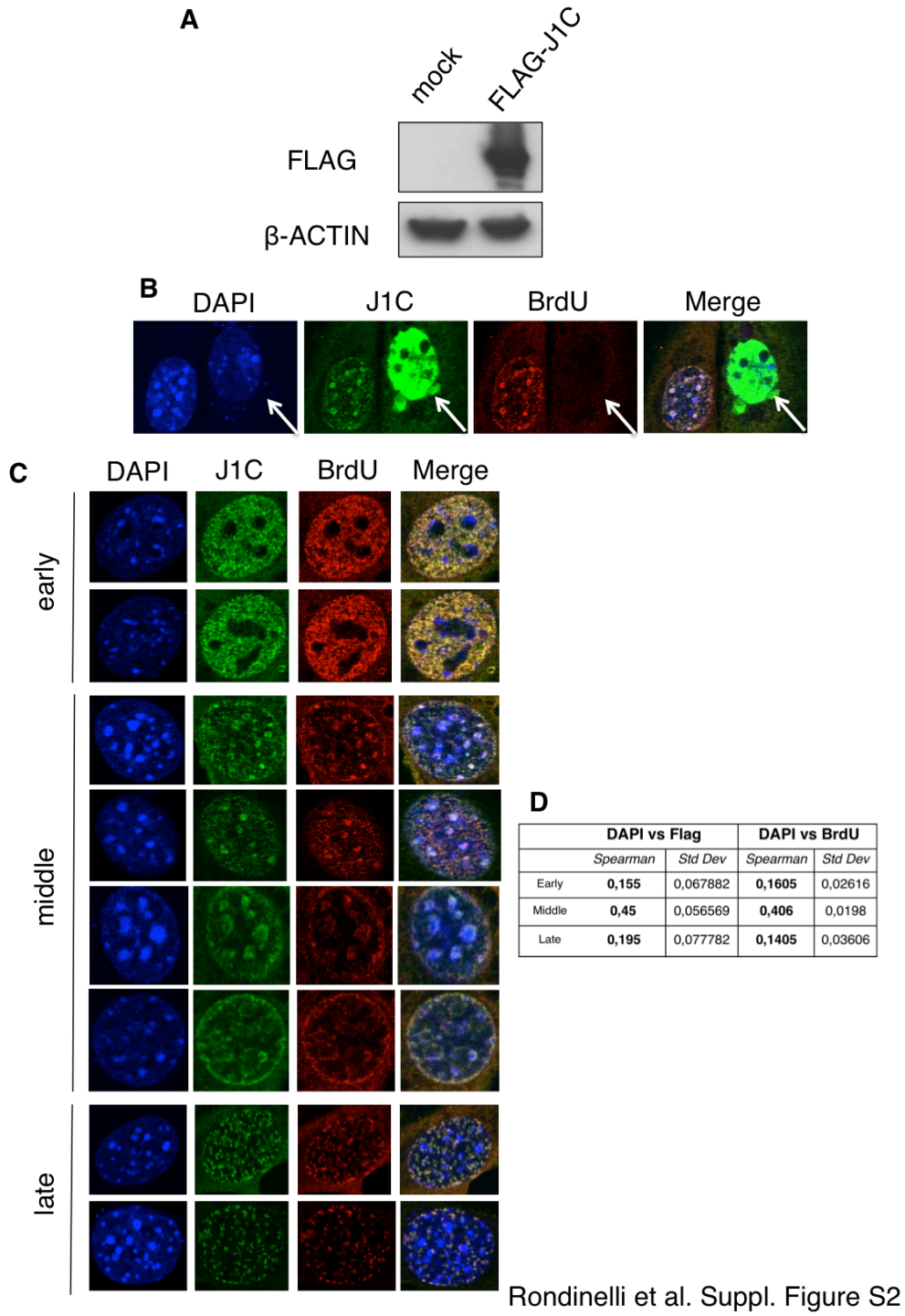

	DAPI vs Flag		DAPI vs BrdU	
	Spearman	*Std Dev*	*Spearman*	*Std Dev*
Early	**0,155**	0,067882	**0,1605**	0,02616
Middle	**0,45**	0,056569	**0,406**	0,0198
Late	**0,195**	0,077782	**0,1405**	0,03606

Figure S2. Confocal analysis of JARID1C colocalization with BrdU and DAPI. **A,** Total lysates from NIH3T3 cells mock transfected or transfected with a flagged-JARID1C plasmid were analysed by Western blotting for Flag-JARID1C and β-ACTIN expression; **B**, Arrows indicates a representative interphase cell expressing Flag-JARID1C; **C,** Representative confocal immunofluorescence images for NIH 3T3 cells transfected with Flag-JARID1C after a BrdU pulse and stained for DAPI, Flag and BrdU. The typical early, middle and late S-phase patterns are shown; **D**, Spearman correlations for DAPI against Flag and for DAPI against BrdU in early, middle and late S phase cells. Three cells per type were analyzed.

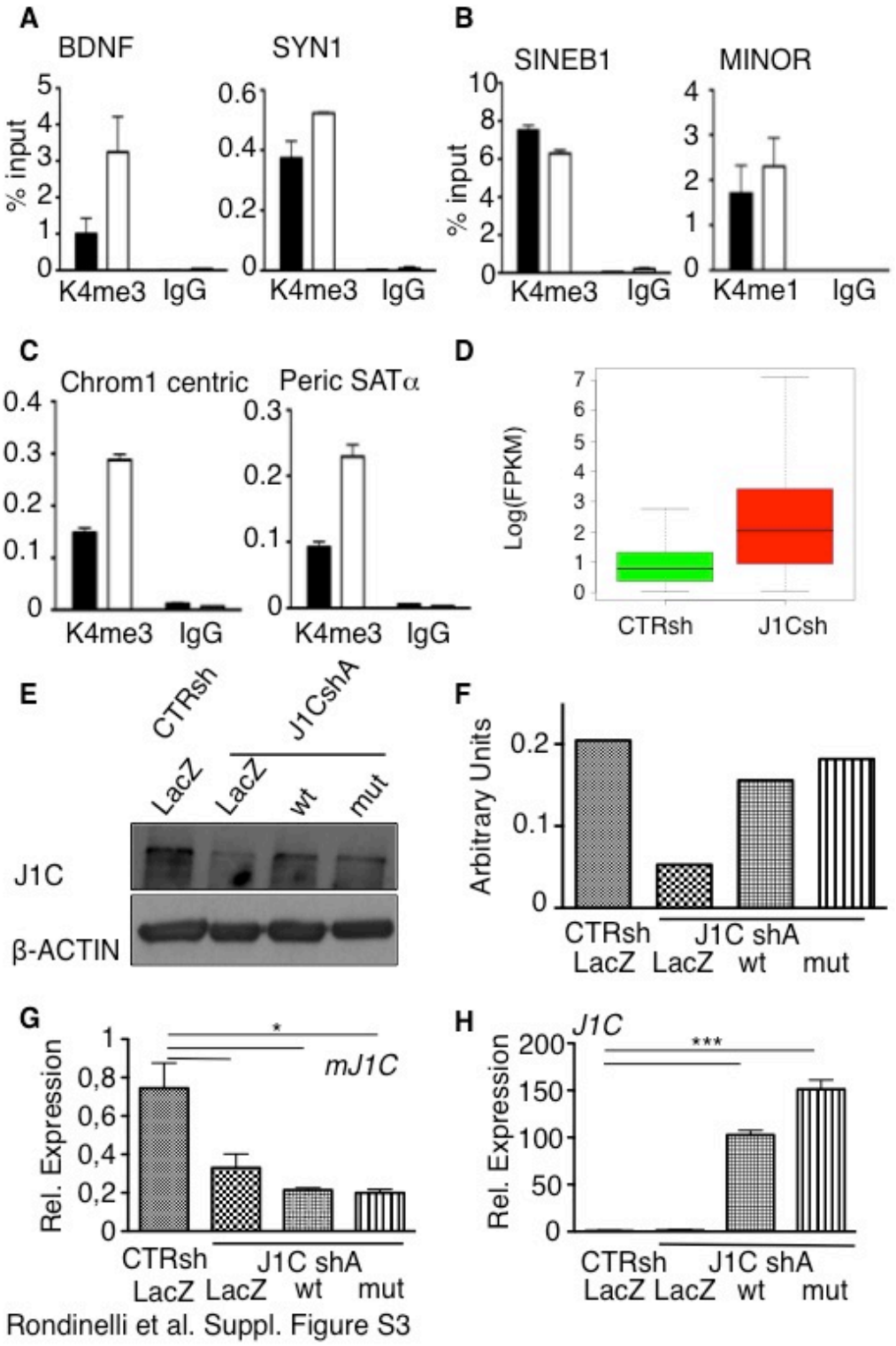

Figure S3. ChIP-qPCR analysis of histone marks of control and JARID1C silenced cells. Western blot analysis and RNA levels of a representative rescue experiment. A, Chromatin from NIH3T3 cells knocked-down for JARID1C expression was immunoprecipitated with anti-K4me3 specific antibody and analyzed by qPCR for enrichment at the BDNF (Brain Derived Neurotropic Factor) and SYN1 (Synapsin 1) promoters. **B**, Chromatin at SINEB1 and minor satellites of control and silenced NIH-3T3 cells was immunoprecipitated with anti-H3K4me3 and anti-H3K4me1 specific antibodies and analysed for enrichment by qPCR with primers listed in Supplemental Methods. Isotipic IgGs were used as controls. Results are

expressed as percentage of input. The error bars represent SEM. **C**, Chromatin from Caki-1 cells knocked-down for JARID1C expression was immunoprecipitated with the indicated antibodies (H3K4me3) and analyzed by qPCR for enrichment at the Chrom1 centric αSAT and Pericentric SATα genomic sequences. Results are expressed as percentage of input. The error bars represent SEM. **D**, Significant increase of H3K4me3 levels in heterochromatic regions (as defined by H3K9me3 enrichment and lack of DNAse sites) in cells knocked-down for KDM5C ($P<1x10^{-16}$)(data from (17)). **E**, NIH-3T3 cells were knocked-down with scrambled (CTRsh) or JARID1C-specific (J1CshA) shRNAs and rescued after 24 hours by transfection of MSCV-LacZ, wt JARID1C or mutant JARID1C (mut) expression vectors. After 48 hours from rescue, total cell lysates were analysed for JARID1C and β-ACTIN expression by Western blotting. **F**, Proteins in blots were quantified using densitometry function of the imageJ software (http://imagej.nih.gov/ij/index.html), normalized to β-ACTIN levels within the same sample and expressed as arbitrary units. **G** and **H,** Total RNA from NIH3T3 rescue experiments was collected to analyse expression of murine J1C (mJ1C, **G**) or human J1C (J1C, **H**) by qRT-PCR. Results are expressed over GAPDH and presented as mean ± SEM of n=3 experiments. *P<0.05 and ***P<0.001 using Student's *t* test.

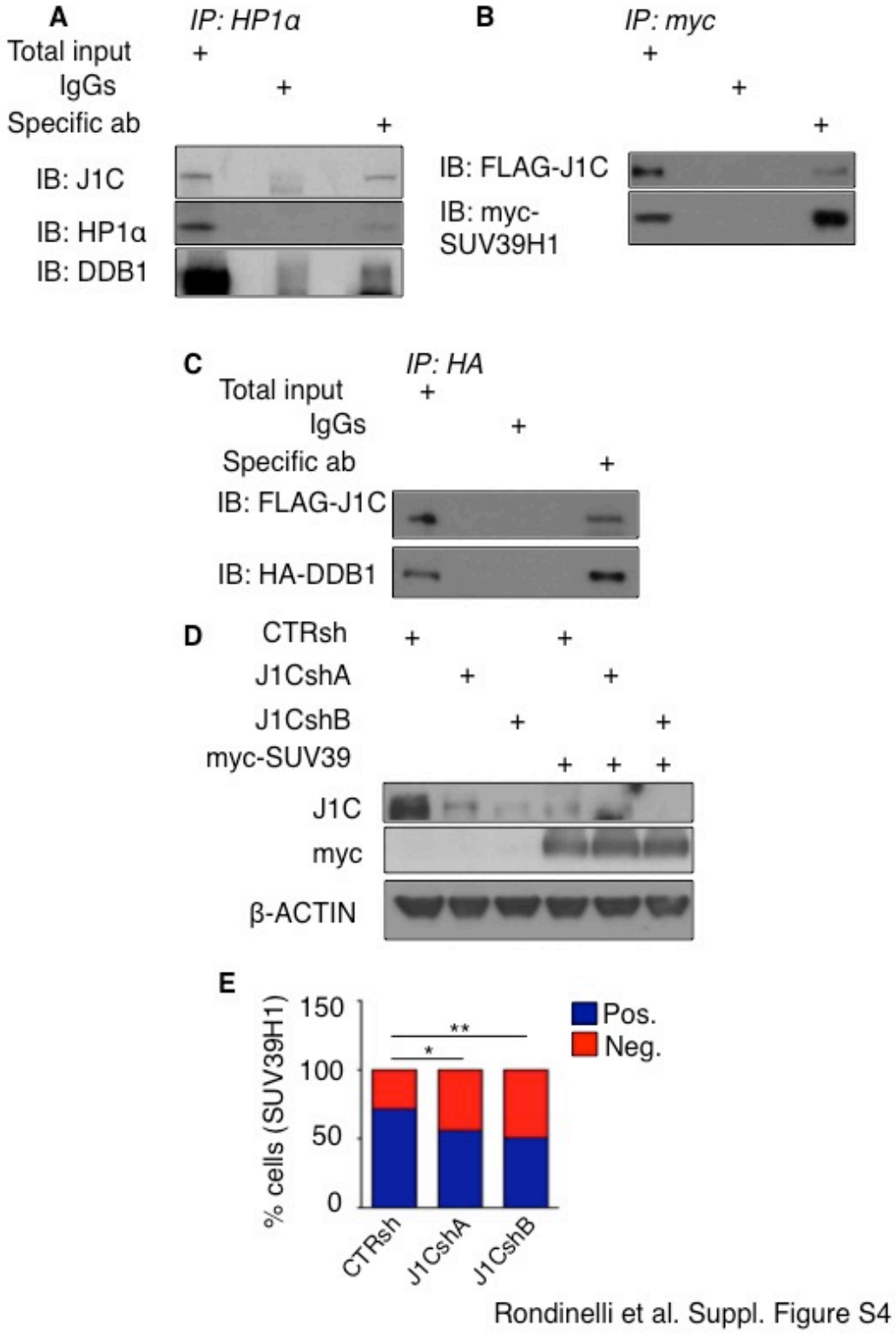

Figure S4. JARID1C interacts with HP1α, SUV39H1 and DDB1 and prevents SUV39H1 localization and chromocentres. A, **B** and **C**, Caki-1 cells were immunoprecipitated in high-salt buffer with the specific indicated antibodies (IP-Abs) or isotypic IgGs as described in Supplemental Methods and loaded on SDS/PAGE gels. Membranes were blotted for the indicated antibodies (IB). 2% of total lysate used in each IP was loaded on gels as Total Input. **D**, Total cell lysates of CTRsh,

J1CshA or J1CshB cells transfected with myc-SUV39H1 were analyzed by Western blot for the expression of JARID1C, myc-SUV39H1 and β-ACTIN. **E,** Quantification of CTRsh, J1CshA and J1CshB cells with (positive) or without (negative) heterochromatic myc-SUV39H1 dots (see representative pictures in Fig. 4) of n=2 independent experiments. About 100 cells per condition were counted in each experiment. $P<0.05$ with Fisher's exact test.

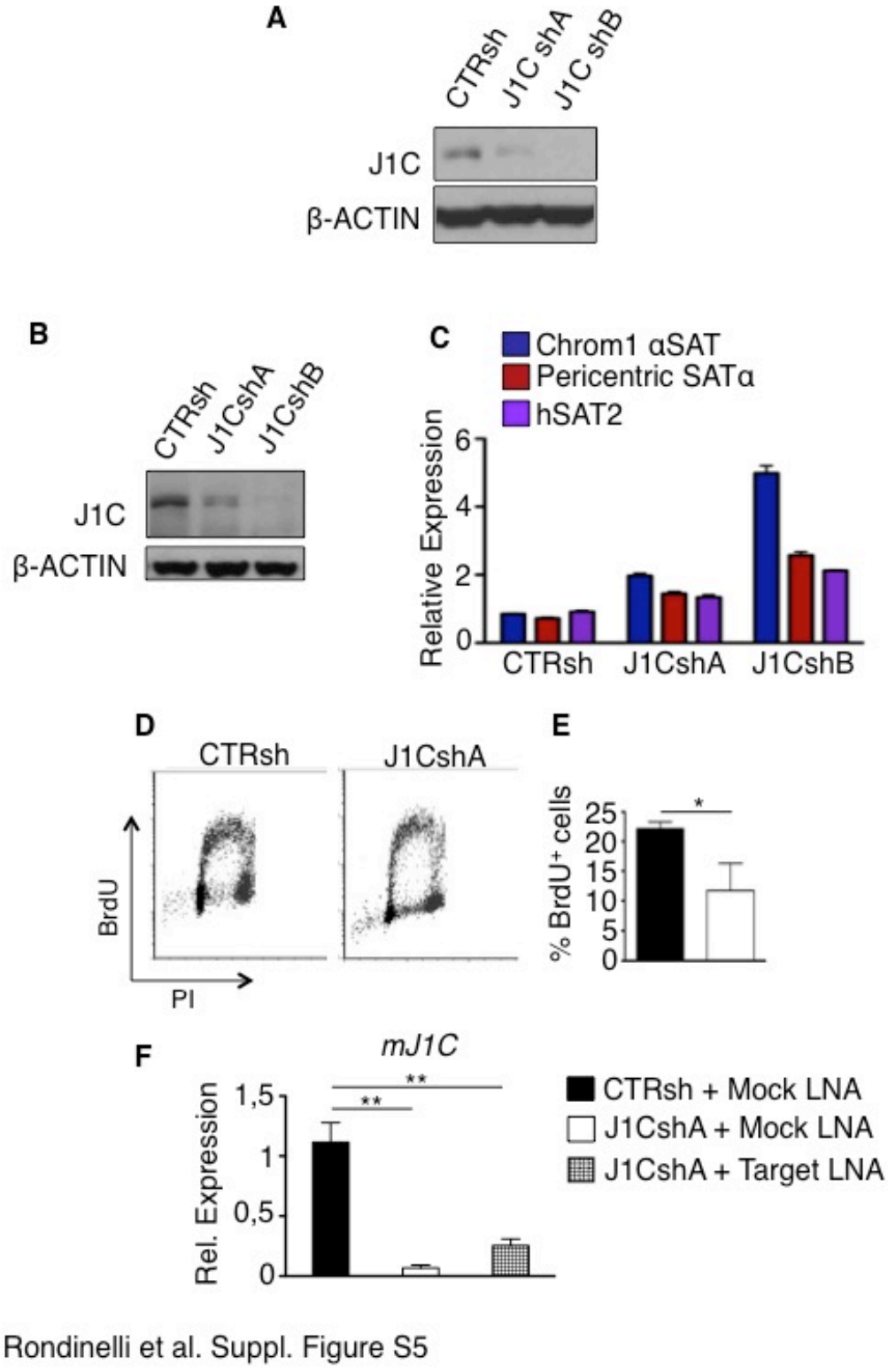

Figure S5. ncRNAs are aberrantly transcribed in NIH-3T3 and Caki-1 cells silenced for JARID1C. MEFs undergo S phase delay and genomic aberrancies upon JARID1C depletion. A, Total cell lysates of NIH3T3 cells were separated on a SDS-PAGE gel and immunoblotted against JARID1C and β-ACTIN. **B,** Western blot analysis of whole cell lysates from scrambled (CTRsh) and JARID1C-silenced

(J1CshA and J1CshB) Caki-1 cells. Membranes were immunoblotted against JARID1C and β-ACTIN. **C,** Total RNA from Caki-1 cells transduced with a scrambled (CTRsh) or J1C-specific shRNAs (J1CshA and J1CshB) was extracted (see Supplemental Methods) and analyzed for the expression of the centromeric Chrom1 αSAT and the Pericentric SATα and hSAT2 ncRNAs. Results are presented as mean ± SEM of one representative experiment of three performed. **D,** Representative PI/BrdU plots of MEFs transduced with scrambled (CTRsh) and J1C-specific (J1CshA) lentiviral vectors; **E,** Quantification of S-phase cells was calculated as described in Supplemental Methods. Results are presented as mean ± SEM of n=3 independent experiments, *P<0.05 with Fisher exact test performed with means of experimental triplicates. **F**, qPCR analysis of mJ1C expression in MEFs transfected with LNAs of experiment in Figure 5D and E. Results are expressed over GAPDH and presented as mean ± SEM of n=3 experiments. **P<0.01 with Student's *t* test.

A

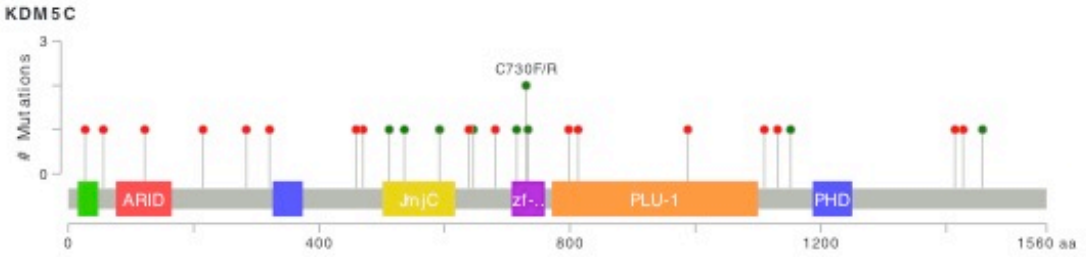

B

Case ID	AA Change	Type	FIS	Cons
TCGA-BP-5202	P27fs	FS del		
TCGA-CJ-4871	F56fs	FS del		
TCGA-B2-5641	E122fs	FS del		
TCGA-CZ-5467	R215*	Nonsense		
TCGA-B0-4828	E284*	Nonsense		
TCGA-AK-3458	F321_splice	Splice		
TCGA-BP-4159	K459*	Nonsense		
TCGA-B0-4694	A470fs	FS del		
TCGA-B0-5106	C512W	Missense	H	mis
TCGA-B0-4816	G536W	Missense	H	mis
TCGA-B0-5077	E592V	Missense	H	mis
TCGA-B0-5108	Y639fs	FS ins		
TCGA-BP-4342	E646D	Missense	H	mis
TCGA-B0-4718	R681*	Nonsense		
TCGA-BP-4803	F715V	Missense	H	mis
TCGA-BP-5169	C730F	Missense	H	mis
TCGA-B0-4844	C730R	Missense	H	mis
TCGA-BP-5190	H733P	Missense	H	mis
TCGA-B0-5094	E798*	Nonsense		
TCGA-BP-5000	Q813*	Nonsense		
TCGA-BP-5189	H988fs	FS del		
TCGA-B0-5698	S1110*	Nonsense		
TCGA-BP-4351	E1131fs	FS del		
TCGA-AK-3430	E1152K	Missense	H	mis
TCGA-CW-5581	D1414fs	FS del		
TCGA-B0-4837	Q1427fs	FS del		
TCGA-B0-4710	R1458W	Missense	L	mis
Case ID	AA Change	Type	FIS	Cons

Rondinelli et al. Suppl. Figure S6

Figure S6. A, Schematic representation of JARID1C (also known as KDM5C) protein with functional domains. Green spikes represent frameshift and nonsense mutations while red spikes represent missense mutations as identified in 417 TCGA-sequenced ccRCC patient samples downloaded from cBioportal (9). X-axis aminoacid number. Y-axis number of total mutations found in sequenced samples. **B**, list of JARID1C mutated samples is reported. The aminoacid change (*AA Change*) and the type of mutation (*Type*) is shown for every patient sample (*Case ID*). For missense

mutations, *FIS* represents the Predicted Functional Impact Score while *Cons* denotes the conservation of the corresponding residue across species (via www. mutationassessor.org).

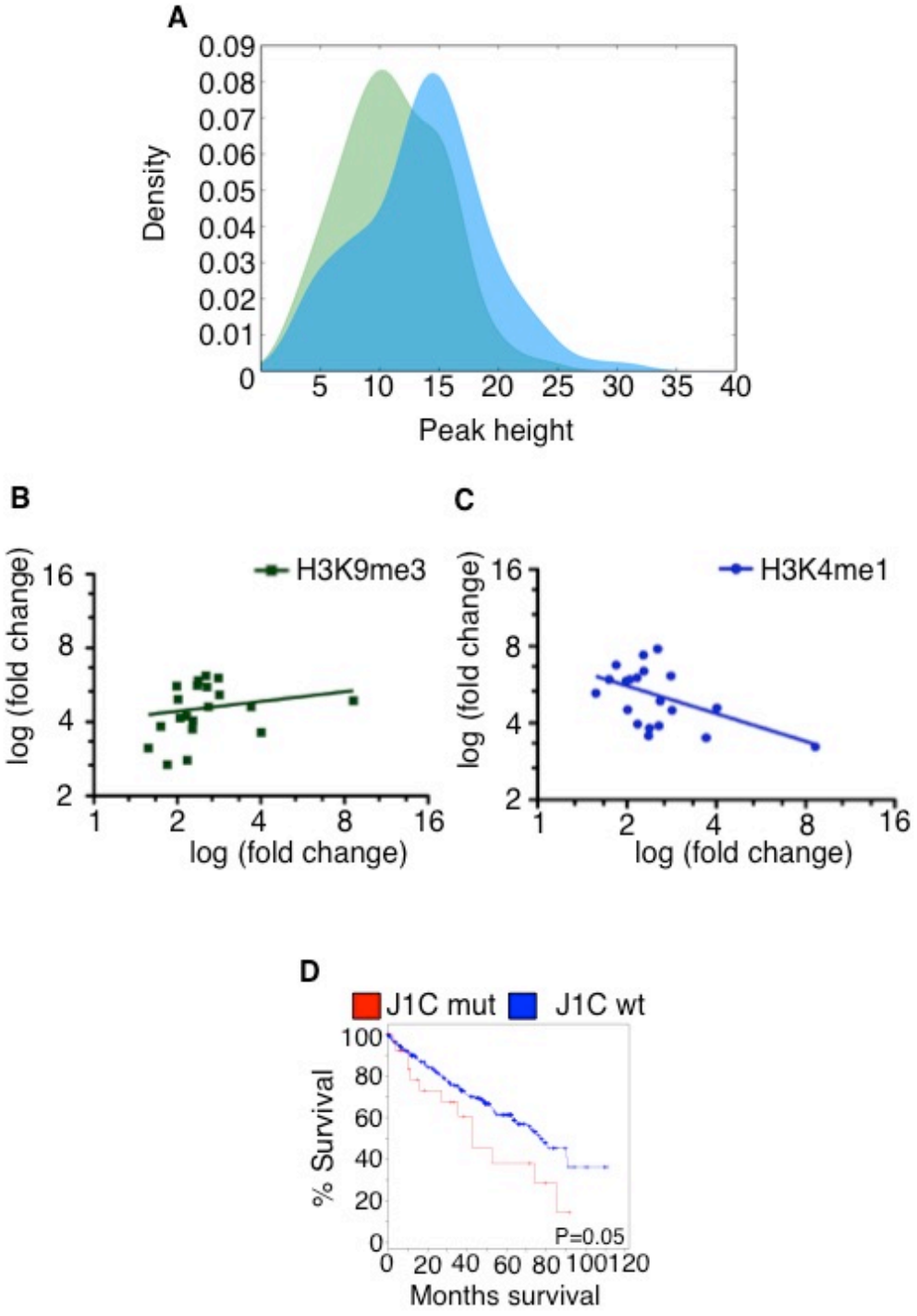

Rondinelli et al. Suppl. Figure S7

Figure S7. A, Density plot of H3K4me1 signals in normal kidney tissue around hyper/hypomethylated loci. The blue curve represents the distribution of peak heights of H3K4me1 signal in an interval ±2500 bp around CpG that are significantly hypomethylated in JARDI1C mutants. Conversely, the green curve represents the distribution of H3K4me1 signals around CpG that are hypermethylated in JARID1C mutants. **B**, Expression of lincRNAs overexpressed in JARID1C-mutated samples versus the corresponding H3K9me3 and **C**, H3K4me1 ChIP-seq peaks in normal

kidney tissue . *x-axis* represents log (fold change) of lincRNA expression, *y-axis* represents the fold enrichment of H3K9me3 and respectively of H3K4me1 ChIP-seq peaks that include ncRNAs dysregulated in JARID1C-mutated ccRCC samples and mapping to both H3K9me and H3K4me1 ChIP-seq peaks (see Supplemental Methods). **D,** Kaplan-Meier survival curves comparing patients harboring wildtype or mutated JARID1C. Data were derived from TCGA (analyzed through http://www.cbioportal.org). P=0.05 with Log Rank significance test.

Ensembl_id	Fold Change	q-value (%)
ENSG00000182057	1,646	4,488
ENSG00000185168	1,894	17,06
ENSG00000203386	2,813	22,294
ENSG00000203645	2,271	0
ENSG00000204362	5,726	0
ENSG00000212930	3,658	0
ENSG00000214145	1,793	0
ENSG00000223387	2,162	0
ENSG00000223410	3,446	17,06
ENSG00000223834	1,765	17,06
ENSG00000223891	1,333	9,709
ENSG00000224037	3,47	9,709
ENSG00000224843	1,489	22,294
ENSG00000225129	2,502	22,294
ENSG00000225285	1,659	17,06
ENSG00000225548	9,479	22,294
ENSG00000225718	2,364	22,294
ENSG00000225794	2,177	17,06
ENSG00000225916	1,696	22,294
ENSG00000225948	4,103	22,294
ENSG00000226782	1,664	17,06
ENSG00000226785	2,381	17,06
ENSG00000226900	5,83	0
ENSG00000227060	1,967	0
ENSG00000227342	9,724	17,06
ENSG00000227634	4,384	0
ENSG00000228223	1,8	0
ENSG00000228271	1,681	22,294
ENSG00000228467	3,589	9,709
ENSG00000229066	8,625	17,06
ENSG00000229118	2,172	4,488
ENSG00000229628	3,797	0
ENSG00000229654	2,385	4,488
ENSG00000229740	4,888	4,488
ENSG00000229891	1,584	22,294
ENSG00000229896	1,971	9,709
ENSG00000230013	2,057	9,709
ENSG00000230096	2,786	9,709
ENSG00000230100	3,419	22,294
ENSG00000230239	2,399	17,06
ENSG00000230975	3,695	17,06
ENSG00000231107	1,571	9,709
ENSG00000231327	1,905	0
ENSG00000231435	2,045	0
ENSG00000231509	2,132	22,294
ENSG00000231826	3,095	9,709
ENSG00000231877	1,68	22,294
ENSG00000231881	5,875	0
ENSG00000232035	3,988	9,709
ENSG00000232080	12,756	17,06
ENSG00000232386	1,743	4,488
ENSG00000233456	1,985	22,294
ENSG00000233521	2,345	9,709
ENSG00000233610	2,313	0
ENSG00000233645	3,355	1,961
ENSG00000234215	1,942	4,488
ENSG00000234292	1,8	4,488
ENSG00000234350	2,053	1,961
ENSG00000234437	1,866	22,294
ENSG00000234580	100,8	9,709
ENSG00000234928	2,461	22,294
ENSG00000235200	3,094	1,961
ENSG00000235215	2,969	0
ENSG00000235597	2,313	4,488
ENSG00000235736	1,835	17,06

Ensembl_id	Fold Change	q-value (%)
ENSG00000236008	1,743	1,961
ENSG00000236030	2,174	17,06
ENSG00000236206	2,133	22,294
ENSG00000236648	26,011	9,709
ENSG00000236751	1,636	17,06
ENSG00000236827	5,41	17,06
ENSG00000236833	2,261	17,06
ENSG00000236990	1,98	22,294
ENSG00000237292	1,952	17,06
ENSG00000237352	3,337	0
ENSG00000237471	3,701	0
ENSG00000237949	3,483	0
ENSG00000238099	1,893	4,488
ENSG00000238290	2,279	4,488
ENSG00000240859	1,975	0
ENSG00000241213	3,098	9,709
ENSG00000241593	1,925	17,06
ENSG00000241599	1,956	17,06
ENSG00000241882	2,881	1,961
ENSG00000243969	4,444	22,294
ENSG00000244791	2,456	22,294
ENSG00000245522	2,028	0
ENSG00000245750	2,537	0
ENSG00000245857	1,873	17,06
ENSG00000247011	1,763	22,294
ENSG00000247993	1,938	17,06
ENSG00000248323	2,247	17,06
ENSG00000248359	2,936	17,06
ENSG00000248373	2,561	0
ENSG00000248767	13,237	9,709
ENSG00000248859	3,406	22,294
ENSG00000249021	2,689	9,709
ENSG00000249153	4,7	17,06
ENSG00000249359	1,744	22,294
ENSG00000249515	45,59	9,709
ENSG00000249951	4,425	9,709
ENSG00000250066	3,961	4,488
ENSG00000250377	5,016	17,06
ENSG00000250390	1,455	22,294
ENSG00000250415	2,657	17,06
ENSG00000250934	2,27	0
ENSG00000251093	3,038	1,961
ENSG00000251176	4,583	9,709
ENSG00000251259	1,212	22,294
ENSG00000251359	1,674	0
ENSG00000251365	1,692	17,06
ENSG00000251580	1,388	22,294
ENSG00000251604	5,325	9,709
ENSG00000253390	1,435	22,294
ENSG00000253433	2,064	17,06
ENSG00000253530	2,77	22,294
ENSG00000253819	5,379	17,06
ENSG00000253844	2,171	0
ENSG00000253986	1,605	9,709
ENSG00000254028	2,038	9,709
ENSG00000254173	4,204	4,488
ENSG00000254235	1,766	22,294
ENSG00000254267	2,055	22,294
ENSG00000254367	2,765	4,488
ENSG00000254427	1,721	17,06
ENSG00000254626	5,171	0
ENSG00000254885	1,999	9,709
ENSG00000254968	2,012	9,709
ENSG00000255146	2,251	0
ENSG00000255314	3,579	22,294

Ensembl_id	Fold Change	q-value (%)
ENSG00000255364	5,856	4,488
ENSG00000255571	6,716	0
ENSG00000255606	2,221	4,488
ENSG00000256001	1,751	22,294
ENSG00000258102	2,855	0
ENSG00000258249	1,672	22,294
ENSG00000258308	1,958	22,294
ENSG00000258332	4,09	4,488
ENSG00000258346	2,624	1,961
ENSG00000258498	4,812	0
ENSG00000258586	1,848	4,488
ENSG00000258600	4,073	17,06
ENSG00000259082	3,421	17,06
ENSG00000259198	1,853	17,06
ENSG00000259203	10,337	9,709
ENSG00000259223	4,015	22,294
ENSG00000259237	7,805	4,488
ENSG00000259309	2,678	17,06
ENSG00000259359	1,428	22,294
ENSG00000259457	2,38	1,961
ENSG00000259579	2,588	0
ENSG00000259604	1,868	17,06
ENSG00000259639	2,839	9,709
ENSG00000259641	1,989	4,488
ENSG00000259703	2,66	4,488
ENSG00000259725	3,316	22,294
ENSG00000260201	2,572	4,488
ENSG00000260219	1,357	9,709
ENSG00000260261	1,892	9,709
ENSG00000260302	2,502	17,06
ENSG00000260432	2,912	0
ENSG00000260492	2,723	1,961
ENSG00000260506	2,624	22,294
ENSG00000260507	1,974	22,294
ENSG00000260620	3,301	4,488
ENSG00000260805	1,322	17,06
ENSG00000260850	7,379	0
ENSG00000260943	1,944	9,709
ENSG00000261257	2,984	9,709
ENSG00000261265	1,754	9,709
ENSG00000261307	4,127	4,488
ENSG00000261319	3,308	17,06
ENSG00000261353	2,319	0
ENSG00000261390	1,838	0
ENSG00000261610	1,989	22,294
ENSG00000261653	2,072	17,06
ENSG00000261706	2,517	1,961
ENSG00000262006	2,663	1,961
ENSG00000262772	4,741	0
ENSG00000263041	15,36	9,709
ENSG00000264215	2,12	4,488
ENSG00000266824	1,707	17,06
ENSG00000267011	1,542	17,06
ENSG00000267079	2,153	1,961
ENSG00000267498	1,378	17,06
ENSG00000267644	2,071	9,709
ENSG00000267666	1,501	22,294
ENSG00000269524	3,017	9,709
ENSG00000269640	1,38	1,961
ENSG00000269927	2,455	17,06
ENSG00000269976	1,873	22,294
ENSG00000270544	3,712	17,06
ENSG00000270996	1,759	4,488
ENSG00000271109	1,371	17,06

Rondinelli et al._Table S1

Table S1. List of lncRNAs differentially expressed between JARID1C-mutated ccRCC versus JARID1C WT ccRCCs. Fold change refers to expression of lncRNAs in J1C-mutated versus J1C WT tumor samples (FDR<0.25).

ID number	ID	Age	Sex	Gene	cDNA Annotation	Protein Annotation
1	PD3289a	57	M	*JARID1C*	c.3385_3386insT	p.D1129fs*75
2	PD3293a	80	M	*JARID1C*	c.807delC	p.T270fs*2
3	PD3302a	53	F	*JARID1C*	c.661G>T	p.E221*
4	PD3357a	71	M	*JARID1C*	c.1935_1936GG>CT	p.E645_E646>D*
5	PD3504a	37	F	*JARID1C*	Exon 4 -4 del(tcagATTGTGGTGGAGGAAG)	
6	PD3515a^	80	M	*JARID1C*	c.1430delA	p.N477fs*2
7	PD3524a	66	M	*JARID1C*	Exon 6 +1 del(CGGAAGAAAGg)	
8	PD3588a	77	F	*JARID1C*	c.3826G>A	p.E1276K
9	PD3580a^	73	M	*JARID1C*	c.4037delA	p.K1346fs*12

Rondinelli et al._Table S2

Table S2. Sample information of primary ccRCC analyzed. A list of the follow up samples analyzed by qPCR for the analysis of ncRNAs from (18) is reported, including the corresponding given number in Fig. 4e and the relative tumor ID as described in (18). Age and sex of patients are included. In addition, the mutation sequenced in the cDNA and the predicted protein product are reported.